

Ceasing of voltage switching amongst graphitic shells in multiwalled carbon nanotubes: A route toward stability

Neha Kulshrestha¹, Abhishek Misra, Reeti Bajpai, Soumyendu Roy, and D. S. Misra

Citation: *Appl. Phys. Lett.* **100**, 043505 (2012); doi: 10.1063/1.3679397

View online: <http://dx.doi.org/10.1063/1.3679397>

View Table of Contents: <http://aip.scitation.org/toc/apl/100/4>

Published by the American Institute of Physics

Ceasing of voltage switching amongst graphitic shells in multiwalled carbon nanotubes: A route toward stability

Neha Kulshrestha,^{1,a)} Abhishek Misra,² Reeti Bajpai,¹ Soumyendu Roy,¹ and D. S. Misra¹

¹*Department of Physics, Indian Institute of Technology Bombay, Mumbai 400076, India*

²*Centre of Excellence in Nanoelectronics, Department of Electrical Engineering, Indian Institute of Technology Bombay, Mumbai 400076, India*

(Received 9 December 2011; accepted 5 January 2012; published online 24 January 2012)

Weakly interacting graphitic shells of different resistivities within multiwalled carbon nanotubes (MWNTs) cause instability in current and thus limit their reliability for electronic device applications. We here demonstrate voltage switching amongst graphitic shells of MWNTs by applying current sweeps with observed switching time in the range of 100–400 ms. We further demonstrate ceasing of this switching behaviour by local metal deposition on the MWNTs. After metal deposition, the graphitic shells behave like resistive wires connected altogether. This concept of metal deposition benefits in the higher conductivity and stable currents for MWNTs and proves their strong candidature as interconnecting wires. © 2012 American Institute of Physics. [doi:10.1063/1.3679397]

Measuring current through nanowires is one of the favorite research topics for theoretical and experimental studies. Carbon nanotubes are the most explored nanostructures for their interesting electrical properties besides the others. Up to now, the electrical properties of single walled carbon nanotubes (SWNTs) and multiwalled carbon nanotubes (MWNTs) are almost fully explored theoretically and experimentally and found favourable for their interconnect applications.^{1–7} In MWNTs several graphitic shells are arranged, forming parallel tubular structures with geometrical arrangement of carbon atoms defining the unique electronic nature of each shell.⁸ SWNTs are easy for modelling the electronic properties of their species; however, practically the MWNTs are preferred candidates for interconnect applications as they are expected to show overall metallic behavior because of the presence of metallic graphitic shells and relatively large diameter (band gap of the semiconducting tubes is inversely proportional to their diameter) as compared to their single wall counterparts which can show both semiconducting or metallic behaviour.

In case of multiwalled carbon nanotubes dispersed on the prefabricated metal electrodes, generally the outermost shell of the tube makes direct contact to the metal electrodes and significantly contributes in the current conduction.^{9,10} The innermost shells couple to the external electrodes through tunneling barriers of different graphitic shells.¹¹ The breakdown of the MWNTs is governed by a power threshold in air as well as in vacuum, after which the oxidation of the shells starts, and breakdown of the tube is initiated through shell by shell failure.⁹ As the resistivities of the shells in MWNTs may correspond to metallic or semiconducting electronic nature, this results in the complexity to explain the experimentally observed electrical characteristics of MWNTs.¹¹ In this letter, we first directly demonstrate the altered resistive paths in MWNTs, through observed voltage switching, and further we present a remedy to overcome the

voltage switching problem by local metal deposition on the tubes. We show that metal deposition on the tubes lead to the improved and stable current values and thus put next step forward for their interconnect application.

In general, the electrical characterization of the carbon nanotubes involves the measurement of electric current flowing through the tube as a result of applied voltage sweeps up to predefined voltage values. The entire literature available for experimental measurement of electrical transport in carbon nanotubes reports the voltage sweep experiments.^{2,9–11} We here demonstrate the voltage switching amongst graphitic shells of multiwalled carbon nanotubes by applying current sweeps. This live switching behaviour can be seen by applying current sweeps up to a fixed value of current and observing the correspondingly developed voltage for every sweep instead of simply measuring the current through the tube by applying voltage sweeps.

The tubes used in these experiments were grown by thermal chemical vapor deposition method using a mixture of ferrocene and toluene (0.1 gm former in 5 ml latter) at a temperature of 850 °C in the heating furnace. Hydrogen has been used as carrier gas (flow of 75 sccm) during the growth. The tubes have been detached from the substrate and ultrasonicated in isopropyl alcohol for several hours for their separation and were dispersed on the prefabricated gold electrodes for electrical characterization. A chromium and gold (Cr/Au) layer of total thickness 250 nm was deposited on Si/SiO₂ (200 nm) for patterning the bottom gold electrodes. The patterns for square contact pads (100 μm × 100 μm) with typical spacing of about 2 μm were obtained by direct writing the spacing lines using electron beam lithography (EBL), on the pre-deposited Cr-Au layer, and using PMMA 950 kA 2% as photoresist. Using wet etching of Cr/Au, the desired spacing between the pads has been fixed. The MWNTs were transferred on the so achieved patterns in order to have them suspended between the two pads. Positions of nanotubes on the gold electrodes were noted down carefully in SEM (Raith 150-TWO from raith GmbH) instrument for the further

^{a)}Electronic mail: nehaphysics@gmail.com.

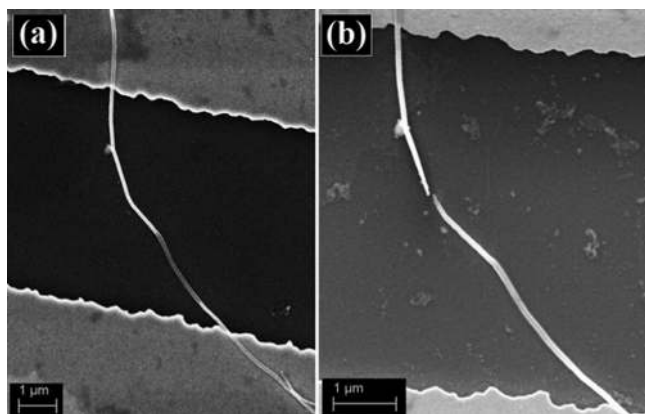


FIG. 1. SEM image of MWNT (a) lying on two gold electrodes, separated by dielectric SiO₂, (b) same tube after current induced breakdown.

steps. Current-voltage (I-V) characteristics of these individual tubes have been obtained using Keithley 4200 source meter in two probe configuration. The SEM image of one individual tube bridging the spacing between two Au electrodes is shown in Figs. 1(a) and 1(b). The current sweep curves

for this tube are shown in Figs. 2(a) and 2(f). Prior to the plotted experimental values, the sample was thermally annealed at 150°C in order to make good contact and avoid any instability in current due to poor electrical contact. After contact annealing, a current sweep of 8 μA has been applied, and the correspondingly developed voltage of 2.5 V was observed in this defined current sweep. In Fig. 2(a) the so obtained curve is shown by black rectangles. For the next current sweep of 15 μA, the voltage suddenly drops from a value of 1.7 V to 0.5 V, and then it continues up to a value of 1.2 V but with a different slope. This sudden decrement in voltage with steep slope indicates that current is now flowing through a different, less resistive path. This curve is shown by 15_1 μA (red circles). To elaborate, the resistance changes from 316 to 74 kΩ for these two paths. Interestingly, the next current sweep of the same value, i.e., the next 15 μA (shown by 15 μA_2, blue triangles), follows the same tract reaching to the same voltage of 1.2 V. With 40 μA current sweep the same tract is visible from the curve. The voltage corresponding to this higher current sweep value (40 μA) has been found to be 2.6 V. To an interesting confirmation, after

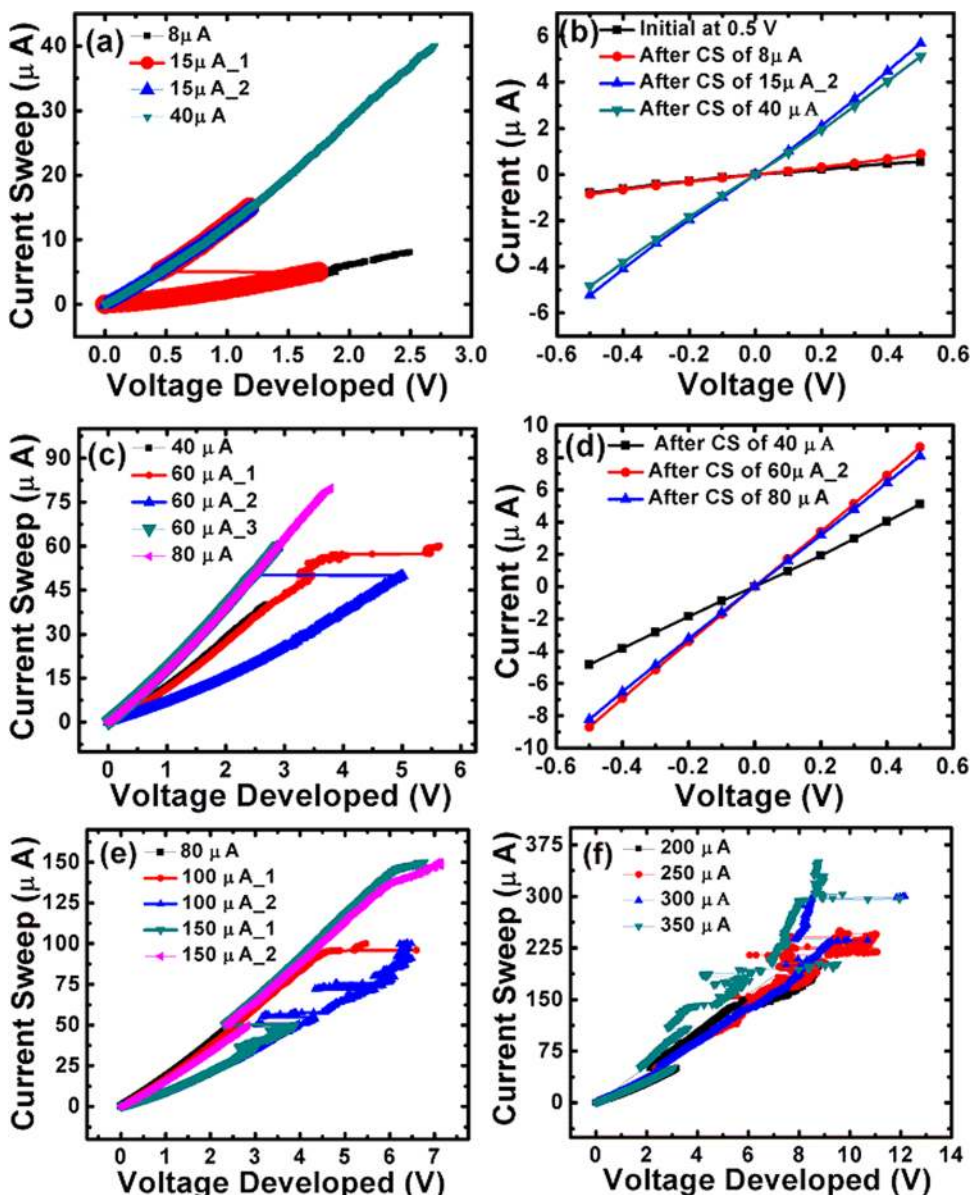


FIG. 2. (Color online) (a)-(f) Current sweep curves of the tube shown in Fig. 1; (a) voltages developed by 8, 15, and 40 μA current sweeps, a clear switching in voltage (from 1.7 to 0.5 V) can be seen for 15 μA_1 current sweep, (b) voltage sweep curves (in the voltage range -0.5 to 0.5 V) taken after different current sweeps, different slopes of the curves support resistivity changes observed in current sweep mode, (c) current sweep curves for 40 to 80 μA current, (d) voltage sweep curves corresponding to (c), (e), and (f) current sweep curves for higher currents (from 80 to 350 μA).

every current sweep, simple voltage sweeps curves (range -0.5 V to 0.5 V) have also been obtained. The curves shown in Fig. 2(b) show the current values corresponding to voltage sweeps. The curve having black rectangles is for the very first voltage sweep taken before any current sweep. These voltage sweep curves support the current sweep obtained data by changing the slopes according to the different resistivities of the paths. In Fig. 2(c) the curves for higher current sweeps are shown. The curve for $40 \mu\text{A}$ is again shown for reference. The voltage developed for the sweep of $60 \mu\text{A}$ shows a switching towards higher voltage side (from 4.5 V to 5.5 V, higher resistive path), and it continues to 5.6 V. For the next current sweep of $60 \mu\text{A}$ again a switching is observed when voltage suddenly decreases from 5 to 2.5 V. The next sweep of $60 \mu\text{A}$ follows the path defined by the previous sweep. The $80 \mu\text{A}$ current sweep follows the similar resistive path. The corresponding voltage sweeps obtained data is shown in Fig. 2(d) which again supports the changed resistive paths defined by current sweeps. The next higher current sweeps are shown in Fig. 2(e) [up to $150 \mu\text{A}$] and in Fig. 2(f) [up to $350 \mu\text{A}$]. Increasing instability of the shells can be seen by the increased fluctuations in voltage at higher current values. After $350 \mu\text{A}$ current sweep, the open circuit voltage developed suggested the breakdown of the tube. The SEM observation (Fig. 1(a)) confirmed the breakdown of the tube. This voltage switching is a direct observation of different resistive nature of the shells of different chiralities within the multiwalled tubes. The switching time (time taken when the current switches from one shell to other shell including simultaneous burning of more than one shells) may be important for evaluating the RC time constant in nano devices fabricated using nanotubes. Towards this approach, we have measured the time taken in switching from one voltage value

to the immediate altered value. It is important to note that the switching time is different for the different resistive changes and lies in the limit of 100 – 400 ms. This measured time is for the current sweeps with a step of $0.1 \mu\text{A}$ and is sensitive to this parameter (current step in program).

Based on the above observations, it is fundamentally possible to observe resistive switching in naturally existing or artificially synthesized two wall nanostructures having different resistivities and can lead to the applications of these nanostructures as molecular switches. But in the applications like interconnects on chip, the current through the wire should be well defined for a particular voltage and should not alter at the same voltage. The isolated graphitic shell structure of MWNTs is therefore an obstruction for their desired interconnect applications. We have observed that metal deposition on a MWNT not only improves its electrical properties but also can be used to cease the observed voltage switching. We here make clear that the metal is deposited at the tube on the site where no beneath metal electrode is present, i.e., the metal is deposited at the part of the tube which lies in the middle between the two gold electrodes. The SEM image of the MWNT, with Pt metal deposition in middle of the tube, is shown in Fig. 3(a). The local metal deposition on the tube has been achieved using electron beam induced deposition (EBID) of Pt by organometallic precursor trimethylmethylcyclopentadienyl-platinum $[(\text{CH}_3)_3(\text{CH}_3\text{C}_5\text{H}_4)\text{Pt}]$. Pt deposition on the tube yields two-fold benefit: one is that the conductance of the tube after Pt deposition increases significantly and the other is that voltage switching disappears. For the tube shown in Fig. 3, the average zero bias conductance before Pt deposition was calculated to be $40.01 \mu\text{S}$ while after Pt deposition it has increased to $95.83 \mu\text{S}$. Thus 140% increased value of conductance has been observed as a result

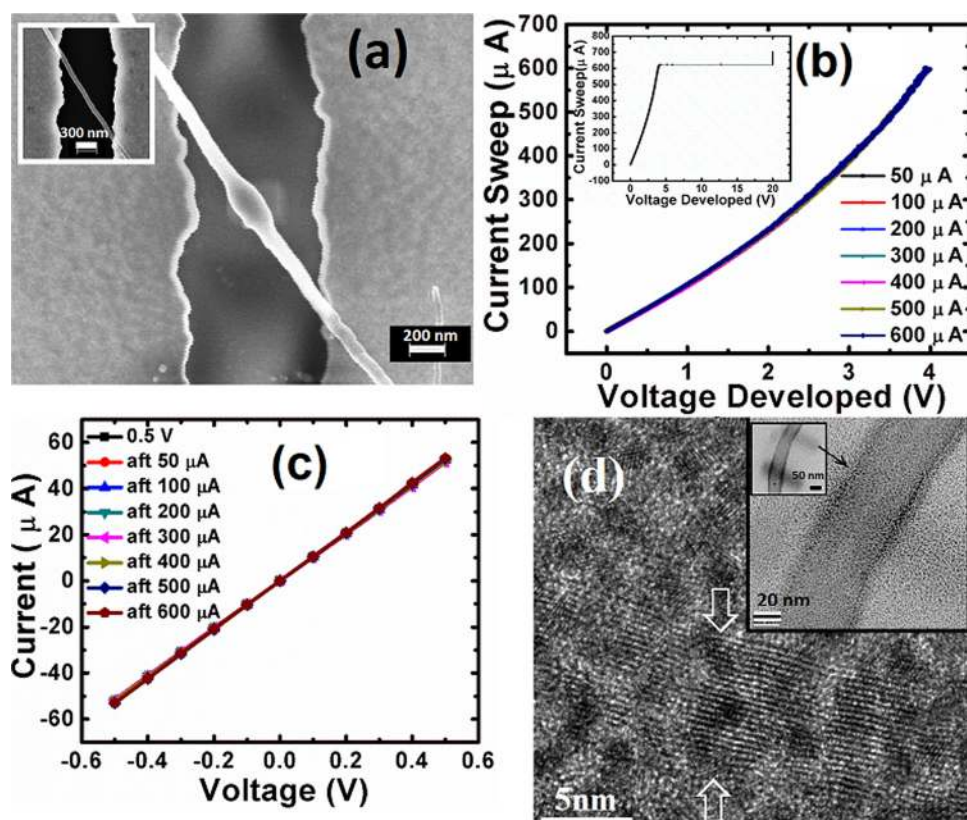


FIG. 3. (Color online) (a) MWNT with Pt deposition at the portion of the tube between the two metal electrodes, the tube before metal deposition is shown in inset. (b) Current sweep curves of the metal deposited tube, no switching has been observed till the breakdown of the tube (breakdown shown in inset). (c) Voltage sweep curves of the tube with metal deposition. (d) HRTEM image of the metal deposited tubes. Arrows are shown to demarcate Pt metal particles intercalated in the graphitic walls of the tube. Inset shows the TEM image of metal deposited tube site.

of metal deposition. We have investigated that the conductance increment comes from the increased density of states (DOS) available for the conduction after metal deposition. This DOS is affected by two reasons: one is the charge transfer between nanotube and metal atoms¹² and the other is radial stress created by the metal deposition on the tube. The first is explained in terms of work function difference, and we have experimentally observed an increment up to 500% after Pt and Tungsten (W) metal deposition on the tubes. Impact of radial stress due to metal deposition on the tube has been experimentally verified by deposition of different thicknesses of metal on the tubes. Thick metal creates more radial stress on the tubes and the band structure of the tube shells being susceptible to the radial stress;^{13,14} hence, thick metal leads to the change in the electronic nature of the shell and in turn the DOS available. But in this study we just report the benefit of the metal deposition to block the voltage switching among the graphitic shells of the tube.

The current sweep experiments were also performed on the metal deposited tubes. In case of metal deposited tube shown in Fig. 3, for the applied current sweeps up to 600 μ A, the curves just overlapped each other as shown in Fig. 3(b), and interestingly no switching has been observed until the breakdown of the tube (shown in the inset of Fig. 3(b)). The voltage sweep curves also overlapped each other, again supporting the current sweeps data. In the similar experiments performed on other tubes, every time switching has been observed for the tubes without any metal deposition while no switching was observed on the metal deposited tubes.

We suggest that this ceasing of switching in metal deposited tubes is caused by metal induced intershell coupling. In our view, Pt atoms of average diameter around 2.45 Å may diffuse within the hexagonal network formed by the carbon-carbon bond length of 1.42 Å. Radial stress on the tube created by deposition of metals also contributes to the increased intershell coupling. The intercalation of metal atoms among the graphitic shells may also be enhanced by the defects present within the tube. It is important to mention here that these results are not specific to Pt metal and similar results are also predictable with other contact metals. However, the amount of improvement will be different for different metals and will depend on the diffusion coefficient of the deposited metal and the amount of stress created by the metal deposition. Diffusion of different metal atoms among the graphitic shells of MWNT is also discussed by Banhart in Ref. 15.

In order to investigate the consequence of metal deposition on the graphitic shell structure of the tube after Pt deposition, HRTEM studies (using JEOL 2100F TEM machine operated at 200 keV) were performed on the multiwalled tubes after deposition of Pt by the same technique reported earlier in this paper. For this, tubes were dispersed on the conventional 200 mesh copper grid. HRTEM investigation of the metal deposited tubes also supports the intershell cou-

pling. The Pt atoms in the nanoclusters deposited by EBID intercalate amongst the graphitic shells of the nanotube, thereby connecting the isolated shells. In Fig. 3(d), the Pt nanoclusters are visible as dark contrast in the image of graphitic walls of the nanotube. It is worthwhile to mention here that the thickness of the deposited metal is controlled by the deposition parameters mainly the element repeated in the experiment. Hence, the parameters used for HRTEM investigation were used so as to produce very thin metal deposition otherwise at the site of deposition; the tube walls are covered by metal clusters, so only dark metal clusters could be viewed (walls were not visible). Hence, the tubes with very thin metal deposition are chosen deliberately to show the HRTEM investigation (Fig. 3(d)).

In summary, sweeping the current (instead of voltage) through the tubes enables us to show the sudden switching in voltage values, indicating the different resistive paths within the tube. We call these abrupt changes in the developed voltage as voltage switching which reflects the isolated shell structure of MWNTs. The important consequence of the metal induced intershell coupling is the absence of voltage switching in MWNTs which confirms the joint state of the various shells caused by metal deposition. High resolution transmission microscopic investigation reveals that after metal deposition MWNTs lose their isolated shell structure and they behave like resistive wires connected altogether at the site of metal deposition.

We acknowledge the Centre for Excellence in Nanoelectronics (CEN) for SEM imaging, lithography, and electrical measurements and Sophisticated Analytical Instrument Facility (SAIF), IIT Bombay for HRTEM imaging.

¹N. Hamada, S. Sawada, and A. Oshiyama, *Phys. Rev. Lett.* **68**, 1579 (1992).

²S. J. Tans, M. H. Devoret, H. J. Dai, A. Thess, R. E. Smalley, L. J. Geerlings, and C. Dekker, *Nature* **386**, 474 (1997).

³T. W. Odom, J. L. Huang, P. Kim, and C. M. Lieber, *Nature* **391**, 62 (1998).

⁴C. T. White and T. N. Todorov, *Nature* **393**, 240 (1998).

⁵B. Q. Wei, R. Vajtai, and P. M. Ajayan, *Appl. Phys. Lett.* **79**, 1172 (2001).

⁶X. Ting, Z. Wang, M. Jianmin, C. Xiaofeng, and T. C. Ming, *Appl. Phys. Lett.* **91**, 042108 (2007).

⁷G. F. Close, S. Yasuda, B. Paul, S. Fujita, and H. S. P. Wong, *Nano Lett.* **8**, 706 (2008).

⁸S. Iijima, *Nature* **354**, 56 (1991).

⁹P. G. Collins, M. Hersam, M. Arnold, R. Martel, and P. Avouris, *Phys. Rev. Lett.* **86**, 3128 (2001).

¹⁰Y. X. Liang, Q. H. Li, and T. H. Wang, *Appl. Phys. Lett.* **84**, 3379 (2004).

¹¹P. G. Collins, M. S. Arnold, and Ph. Avouris, *Science* **292**, 706 (2001).

¹²Y. L. Kim, B. Li, X. An, M. G. Hahn, L. Chen, M. Washington, P. M. Ajayan, S. K. Nayak, A. Busnaina, S. Kar, and Y. J. Jung, *ACS Nano* **3**, 2818 (2009).

¹³B. Shan, G. W. Lakatos, S. Peng, and K. Cho, *Appl. Phys. Lett.* **87**, 173109 (2005).

¹⁴Y. Umeno, T. Kitamura, and A. Kushima, *Comput. Mater. Sci.* **30**, 283 (2004).

¹⁵F. Banhart, *Nanoscale* **1**, 201 (2009).